Civil Engineering Infrastructures Journal xx,xx
DOI: 10.22059/ceij.2026.409331.2472

Seismic Response Analysis of Concrete-Filled Steel Tubular T-Joints Under Repeated Loading Conditions

Taghi Mofid[1*], Al-Sharea[2]

[1] Assistant Professor, Department of Civil Engineering, Urmia University of Technology, Urmia, Iran

[2] Master's graduate, Department of Civil Engineering, Urmia University of Technology, Urmia, Iran

[*]Corresponding Author: Mofid.t@uut.ac.ir

[*]Corresponding Author ORC ID : https://orcid.org/0000-0002-0498-2553

Received: 03/01/2026
Revised: 03/05/2026
Accepted: 05/08/2026

Abstract

Concrete-filled steel tubular (CFST) T-joints are advanced structural components used in bridges, offshore platforms, and high-rise buildings. This study conducted a parametric analysis on eight square-section CFST T-joints under seismic loading using Abaqus software. The numerical models were validated against experimental data from the literature, showing good agreement (within 6.2% for ultimate load). The hysteresis behavior was evaluated based on ultimate load, deflection, stiffness, ductility (μ=2.8–4.2), and energy dissipation (ζ_{hyst}=8.5–12.3%). Key parameters investigated included core concrete strength (30–60 MPa), brace wall thickness (4.2–6 mm), and brace section dimension (60–100 mm). Results indicate that increasing the brace dimension by 66% raises ultimate capacity by 67% and reduces maximum displacement by 39–55%. In contrast, a 43% increase in brace wall thickness yields only a 7.5% capacity gain. Doubling concrete strength increases capacity by 11%. The novel contribution of this study is the systematic comparison of these three design parameters, revealing that brace dimension is the most effective variable for enhancing seismic performance. Thus, the most effective measures for improving load-bearing capacity are, in order: increasing the brace dimension increasing concrete strength increasing brace wall thickness.

Keywords: Concrete-filled steel tube (CFST); Chord-brace joint; Finite element analysis (FEA); Seismic behavior; Cyclic loading.

Nomenclature:	
b_0 = chord width (mm)	
b_1 = brace width (mm)	t_0 = chord wall thickness (mm)
f_{cu} = concrete compressive strength (MPa)	t_1 = brace wall thickness (mm)
L_0 = chord length (mm)	μ = ductility index
L_1 = brace length (mm)	ζ_{hyst} = equivalent viscous damping ratio (%)

1. Introduction

Concrete-filled steel tubular (CFST) members have become integral components in the construction of modern infrastructure, prominently featuring in long-span bridges, high-rise buildings, and advanced truss systems (Ali & Mahdi, 2025; Liang & Han, 2025). Their composite nature, melding the compressive strength of concrete with the ductile properties of steel, confers significant structural advantages, including (Labibzadeh et al., 2024; Xiong et al., 2025). Among CFST applications, T-joints play a pivotal role, where the performance of these connections significantly influences both structural safety and engineering costs (Ghandi et al., 2025; Xie et al., 2025). These joints are formed by connecting steel tubes filled with concrete, creating a composite system that combines the high strength and ductility of steel with the durability and fire resistance of concrete (Ghassemieh et al., 2017; Xiong et al., 2024). The performance of CFST joints is influenced by various factors including the material properties of steel and concrete, joint geometry, and construction details. Proper design and detailing of CFST joints are essential to ensure the overall structural integrity and load-carrying capacity of CFST structures. The behavior of CFST joints under different loading conditions, such as axial compression, bending, and seismic forces, can significantly affect the overall performance and safety of CFST structures. Therefore, a comprehensive understanding of the behavior and design principles of CFST joints is crucial for the successful implementation of CFST structures in various engineering applications. Accordingly, understanding the seismic behavior of CFST joints, particularly under reversed cyclic loading representative of earthquake actions, is thus vital for the safe and cost-effective design of critical structures. Understanding the cyclic degradation behavior of structural components under reversed loading is essential for seismic design. In this regard, experimental studies on reinforced concrete members (Mofid & Tavakoli, 2021, 2023; Omranian et al., 2023) have provided valuable insights into stiffness degradation and energy dissipation under periodic loading, which are also relevant to CFST joints subjected to seismic actions. While numerous experimental and analytical studies have been conducted to evaluate their static performance, there remains a pressing need for comprehensive numerical investigations that capture the complex, hysteretic, and nonlinear responses of CFST joints during strong ground motions. For composite and hybrid structural systems, including CFSTs, seismic demands are further complicated by the interaction of constitutive behaviors (e.g., concrete cracking, steel yielding, bond-slip phenomena), as well as by the influence of joint geometry, material nonlinearity, and local failure mechanisms (Abedini et al., 2025; ISLAM et al., 2024; SHAHRIARI & JAVAHERI, 2017; Zhang et al., 2024).

Recent studies have highlighted the need for three-dimensional, nonlinear finite element models that can accommodate the multiaxial stress interactions and hysteretic energy dissipation characteristic of actual earthquake scenarios. CFST T-joints are subjected to complex internal forces during seismic events, including bending, shear, and axial loads. The steel tube provides confinement to the concrete core, delaying local buckling and enhancing ductility, while the concrete core shares compressive stresses and restrains inward buckling of the steel wall. Under cyclic seismic loading, this composite action is mobilized repeatedly, leading to cumulative damage in both materials. The flexural capacity of the chord, which is central to T-joint performance, is especially critical as it dictates the ability of the joint to sustain inelastic deformations without catastrophic failure. CFST T-joints are widely used in practical engineering applications, including offshore platform structures, long-span bridge trusses, high-rise building moment-resisting frames, and wind turbine support towers. In these applications, the joints are often subjected to reversed cyclic loading during seismic events, making their hysteretic behavior and energy dissipation capacity critical for overall structural safety. The remainder of this paper is organized as follows. Section 2 presents a critical review of previous studies on CFST joints. Section 3 describes the numerical modeling methodology, including material properties, element selection, contact definitions, and boundary conditions. Section 4 validates the numerical model against experimental data. Section 5 presents the parametric analysis results, including the effects of concrete strength, brace wall thickness, and brace dimension on hysteresis behavior, ductility, and energy dissipation. Section 6 discusses the practical implications, compares results with design codes, and identifies study limitations. Finally, Section 7 summarizes the main conclusions and recommendations for future work.

2. Literature Review

The behavior of Concrete-Filled Steel Tubular (CFST) joints, particularly T-joints, has been the subject of numerous experimental, numerical, and analytical studies. This section critically reviews previous research, organized thematically, to identify the research gap addressed by the present study.

2.1 Experimental studies on CFST joints

Early experimental investigations focused on the static and fatigue behavior of hollow section joints, establishing a baseline for understanding the role of concrete infill. Mashiri and Zhao (Mashiri & Zhao, 2010) conducted fatigue tests on square hollow section (SHS) T-joints with concrete-filled chords. Their key finding was that cracking initiates at the weld toe between the brace and chord under in-plane tensile fatigue loading, and that concrete infill significantly delays crack propagation. Huang et al. (Huang et al., 2018) experimentally investigated the joint resistance and failure modes of CFST truss girders. They found that concrete filling prevents chord face failure, shifting the failure mode to punching shear, thereby increasing the joint capacity. Yang et al. (Yang et al., 2024) tested 12 T-shaped composite joints with double-skin concrete-filled chords and hollow braces. Their results showed that increasing the brace-to-chord diameter ratio (β) from 0.3 to 0.5 significantly increased the load-bearing capacity of the specimens, highlighting the importance of brace dimension.

2.2 Numerical and analytical modeling approaches

Numerical simulations have been widely used to complement experimental studies and to explore a wider range of parameters. Nassiraei et al. (Nassiraei et al., 2016) performed numerical analyses on T- and Y-shaped CFST joints with collar plate reinforcements. They concluded that the ratio of brace diameter to chord diameter (β) and the brace-to-chord thickness ratio (τ) have a significant impact on the ultimate strength and failure mode of reinforced connections compared to unreinforced ones. Xie et al. (Xie et al., 2019) developed a finite element (FE) model of a CFST K-joint and studied its ultimate bearing capacity. Their results revealed that the load-displacement curves of CFST K-joints can be divided into three distinct stages: elastic, elastic-plastic, and failure. Montuori et al. (Montuori et al., 2024) introduced a new FE modeling approach to simulate the behavior of CFST members under cyclic bending. Their proposed model was able to accurately detect failure, the number of cycles leading to failure, and subsequent failure modes, demonstrating the capability of advanced FE methods for seismic simulations. In the context of seismic analysis, the rotational component of ground motion has been recognized as a critical factor in crack propagation studies, as shown in the dynamic analysis of RCC dams (Tavakoli et al., 2023). Although focused on dams, such findings underscore the need for comprehensive seismic models that incorporate multi-component ground motions in the assessment of CFST joints.

2.3 Design code comparisons and analytical models

Several studies have compared the predictions of different design codes and proposed analytical models for CFST members. Hassam et al. (Hassam et al., 2024)presented a comparative analysis of different CFST strengthening schemes, evaluating the design methods specified in AISC (2016), EC4 (2004), CECS (2004), and GB (2019) codes. They found significant discrepancies among code predictions, particularly for special-shaped CFST sections. Lan et al. (Lan et al., 2024) provided a comprehensive review of computational methods for key parameters of force-displacement relationships in CFST beam-column connections. Their key conclusion was that no single method can accurately calculate the deformation capacity of all connection types, indicating the need for further research. Pinto and Fonseca (Pinto & Fonseca, 2024) investigated the mechanical behavior of high-strength CFST members, clarifying the important role of the steel tube in creating passive confinement that limits crack propagation and increases concrete ductility.

2.4 Research gap identified from the literature

Despite the substantial body of research summarized above, several critical gaps remain. First, most numerical studies on CFST T-joints have focused on static or monotonic loading, with limited attention to full reversed cyclic loading representative of earthquake actions. Second, while individual parameters such as concrete strength or brace thickness have been studied, a systematic comparison of the relative effectiveness of different design parameters (brace dimension, wall thickness, concrete strength) on the complete hysteresis response (including ductility and energy dissipation) is lacking. Third, few studies have quantified key seismic performance indicators such as the ductility index (μ) and equivalent viscous damping ratio (ζ_{hyst}) for CFST T-joints. Fourth, the interaction effects between parameters (e.g., whether the benefit of larger brace dimensions is amplified by thicker steel walls) have not been thoroughly examined. The present study addresses these gaps by conducting a parametric numerical investigation of eight CFST T-joint models under cyclic loading, with a focus on extracting hysteresis parameters, comparing parameter effectiveness, and providing practical design recommendations.

3. Numerical Analysis Methodology

The T-shaped connection model under investigation was inspired by the connections of large bridges. The general view of this connection and the details of the T-shaped connection are presented in Figures 1 and 2.

Figure 1. Overview of the CFST T-joint used in the bridge structure

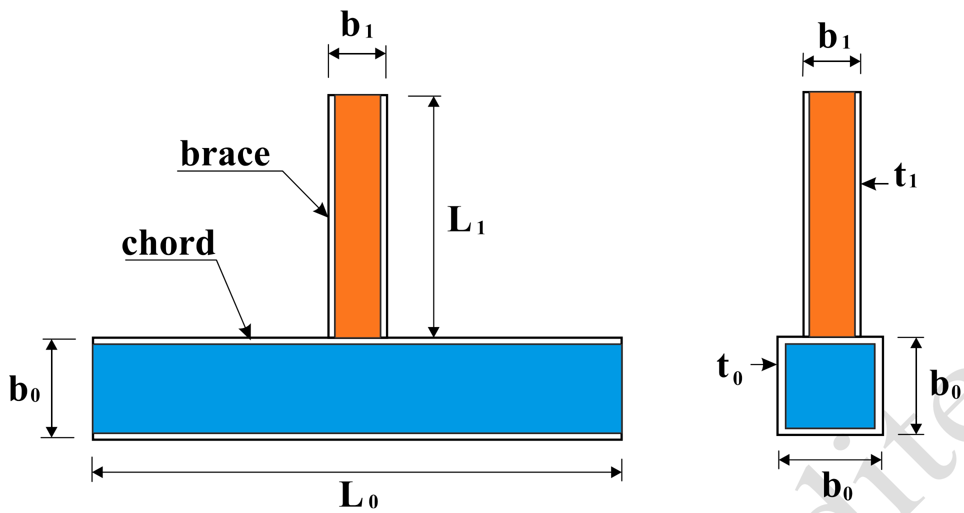

Figure 2. Geometry details of T-joint with square cross-section in chord and brace

It should be noted that the brace (vertical member) and chord (horizontal member) sections in this joint are made of steel and both are hollow. The aim of this study is to model the change in behavior and load-bearing capacity of the joint by embedding the concrete element section inside the steel element. Abaqus/CAE FE software was used to model and analyze the joint. In this analysis, two types of failure modes were considered, both of which can be captured:

- Ductile failure mode: In this mode, only tensile members are considered in the failure mechanism. In this scenario, the forces associated with the members effective in the failure mechanism are calculated through equilibrium and plasticity relations.
- Brittle failure mode: In this mode, only compressive elements are considered in the failure mechanism and the collapse resistance of the connection is determined when the first compressive member is damaged. Therefore, an accurate elastoplastic buckling model is necessary to evaluate the ultimate strength of the connection, which is usually observed at small displacements.

A set of eight chord-brace CFST T-shape joints were modeled. The elements in the joint modeling consisted of two parts: the core concrete and the steel tube. The concrete was modeled using 8-node solid elements C3D8R, and the steel member was modeled using 4-node shell elements S4R. For steel sections, a yield stress of 335 MPa and an elastic modulus of 211 GPa were defined. Also, a density of 7850 kg/m^3, a plastic strain of 0.22, and a Poisson's ratio of 0.3 were considered for steel. Concrete with two strength grades of 30 MPa and 60 MPa were modeled. For C30 and C60 concrete sections, Poisson's ratio of 0.18 and 0.2 and densities of 2300 and 2400 kg/m^3, respectively, were used. The Young's modulus of concrete with a compressive strength of 30 and 60 MPa was also determined to be 25 and 33 GPa, respectively. Besides, rigid steel support plates with a Poisson's ratio of 0.3 and a Young's modulus of 1000 GPa were modeled to prevent deformation at the supports and loading point. Table 1 reports the geometric characteristics of this joint.

Table 1. Geometric characteristics of the CFST T-joint models

Model ID	L_0	b_0 (mm)	t_0 (mm)	L_1 (mm)	b_1 (mm)	t_1 (mm)	f_{cu} (MPa)
TCJ-1	740	120	3.5	320	60	4.2	30
TCJ-2	740	120	3.5	320	60	6.0	30
TCJ-3	740	120	3.5	320	100	4.2	30
TCJ-4	740	120	3.5	320	100	6.0	30
TCJ-5	740	120	3.5	320	60	4.2	60
TCJ-6	740	120	3.5	320	60	6.0	60
TCJ-7	740	120	3.5	320	100	4.2	60
TCJ-8	740	120	3.5	320	100	6.0	60

The interaction between steel and concrete was defined by assembling the created parts and assigning the Mohr-Coulomb friction constraint in the vertical direction based on surface-to-surface contact. In this way, several master and slave surfaces were determined, where concrete acts as a slave surface and steel as the master surface. This choice was made due to the fact that concrete is softer and its matrix is finer than steel, which can significantly reduce the error margin. Regarding the interaction, there are two options in Abaqus, finite sliding and small sliding. The choice between the finite and small sliding options depends on the nature of the contact behavior in the analysis. For scenarios involving significant displacements, finite sliding is more appropriate and ensures that the changing contact geometry is accurately modeled. In contrast, for applications where movements are minimal, small sliding offers a simpler and faster solution while maintaining sufficient accuracy. Accordingly, in this study, there was a possibility of small sliding between the coupling surfaces in the friction model. Therefore, the shear force was calculated through the friction coefficient and tangential pressure. The effect of friction with a coefficient of 0.2 between the steel and concrete surfaces was considered. The mechanical and strength characteristics of steel and concrete defined in the Abaqus software were input according to Tables 2 and 3.

Table 2. Properties of steel tube

Material	Yield strength (MPa)	Tensile strength (MPa)	Elastic modulus (GPa)	Poisson's ratio	Plastic strain	Density (kg/m^3)
S355	335	497	211	0.3	0.22	7850

Table 3. Properties of core concrete

Material	Compressive strength (MPa)	Elastic modulus (GPa)	Poisson's ratio	Density (kg/m^3)
C30	30	25	0.18	2300
C60	60	33	0.20	2400

To apply boundary conditions to the joint, the ends of the chord was considered as hinged supports. The axial compression load to the chord member was applied and kept constant during the loading process. In addition, the free end of the brace was considered for applying the vertical reversed cyclic load along the brace longitudinal axis. The cyclic load was applied in two steps, following the recommendation of (Varma et al., 2004) that was extracted from the guidelines of the applied technology council ATC-24 implemented for cyclic tests of steel members. Figure 3 demonstrates the load and boundary conditions of the CFST T-joint models.

Bond-slip behavior at the steel-concrete interface was not explicitly modeled in this study. This simplification is justified because (1) the steel tube provides passive confinement to the concrete core, which primarily relies on normal compressive contact rather than tangential bonding; (2) the primary failure modes of interest are steel yielding and concrete crushing, not interfacial debonding; and (3) previous CFST modeling studies(Han, 2024; Varma et al., 2004); have shown that perfect bond assumption yields acceptable accuracy for global hysteresis response. The friction coefficient of 0.2 was selected based on the recommendation of Li et al (Li et al., 2021) for steel-concrete interfaces in CFST models.

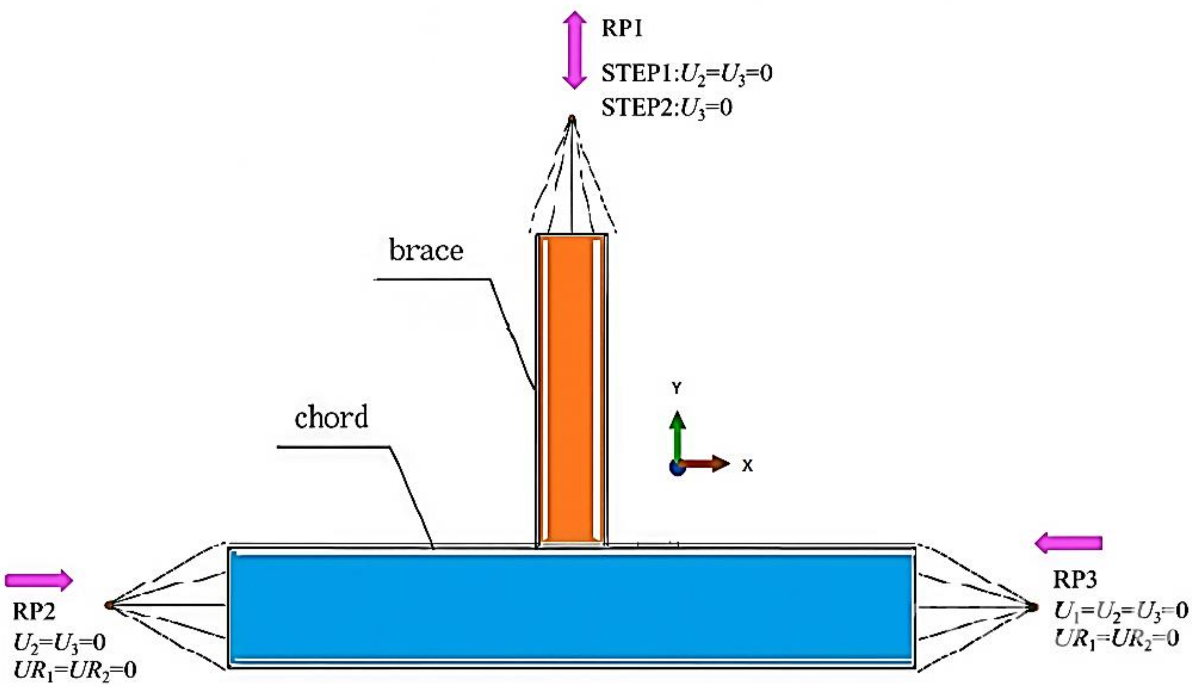

Figure 3. Load type and boundary conditions of CFST T-joint model

4. Model Validation

To validate the accuracy of the numerical modeling approach, a reference CFST T-joint specimen from the experimental study by (Varma et al., 2004) was simulated using the same meshing, material properties, contact definitions, and boundary conditions described in Section 3. The experimental hysteresis load-displacement envelope was compared with the numerical predictions. The results showed good agreement, with a maximum difference of 6.2% in ultimate load and 5.8% in initial stiffness. This level of discrepancy is acceptable given the simplifications in material modeling (e.g., assuming perfect bond without slip, using average rather than measured material properties).

Regarding nonlinear modeling details: (1) Material nonlinearity was considered through elastic-plastic steel behavior with isotropic hardening and concrete damaged plasticity (CDP) model for compressive crushing and tensile cracking. (2) Geometric nonlinearity was activated in Abaqus using the NLGEOM option to account for large displacements and finite strains. (3) Contact nonlinearity was modeled using surface-to-surface contact with a hard contact pressure-overclosure relationship in the normal direction and a penalty friction formulation in the tangential direction ($\mu = 0.2$). (4) Solution controls included automatic incrementation with a maximum increment size of 0.05, a minimum increment size of 10^{-6}, and a maximum number of iterations of 20 per increment. The convergence criterion was set to 0.5% residual force norm.

5. Numerical Parametric Analysis Results

This section discusses the effect of changes in core concrete compressive strength, brace member wall thickness, and brace member section dimension on the overall CFST T-joint ultimate load and deflection, joint stiffness, ductility, and energy absorption.

5.1 Practical implications for real structures

The results indicate that for real-world seismic design applications, increasing the brace cross-sectional dimension is the most efficient strategy to enhance load capacity and energy dissipation. In practice, this can be achieved by selecting larger brace sections without necessarily increasing wall thickness, which provides only marginal benefits. For bridge trusses and offshore platforms where weight is a concern, a larger but thinner-walled brace (e.g., $b_1 = 100$ mm, $t_1 = 4.2$ mm) is recommended over a smaller but thicker-walled section (e.g., $b_1 = 60$ mm, $t_1 = 6$ mm). Additionally, conventional concrete (C30) is sufficient for most applications, as higher-strength concrete (C60) provides only an 11% capacity increase at significantly higher material cost. These recommendations can guide cost-effective seismic retrofitting and new construction of CFST T-joints.

5.2 Effect of Core Concrete Strength

The effect of concrete strength on the capacity of T-shaped composite joints is discussed. The hysteresis load-displacement diagram comparison of the numerical joint models is shown in Figure 4. It is worth noting that no significant changes were observed in the load-bearing capacity of T-shaped joints by increasing the compressive strength of concrete from 30 MPa to 60 MPa. Thus, it can be argued that the capacity of these joints can be increased and the amount of energy absorbed in retrofitting designs can be improved by using lower-strength concrete types. In this regard, the ultimate bearing capacity of the TCJ-1 model (with 30 MPa concrete) is 108.4 kN, while the TCJ-5 model (with 60 MPa concrete) reaches 120.5 kN. This represents an 11% increase in bearing capacity when the concrete compressive strength is doubled from 30 to 60 MPa. The limited 11% capacity increase is attributed to the fact that in CFST T-joints, the steel tube yields before the concrete reaches its full compressive strength. The concrete's role is primarily to provide passive confinement and delay local buckling, rather than directly resisting the applied load. Thus, beyond a certain threshold, higher concrete strength yields diminishing returns. This indicates that the concrete used does not need to be of a special high-strength type and that conventional concretes can also be used to strengthen the CFST T-joints.

5.3 Effect of Brace Wall Thickness

The effect of changing the brace wall thickness in the T-shaped connection and its effect on the load-bearing capacity, ductility, and overall energy absorption of the connection is investigated in this section.

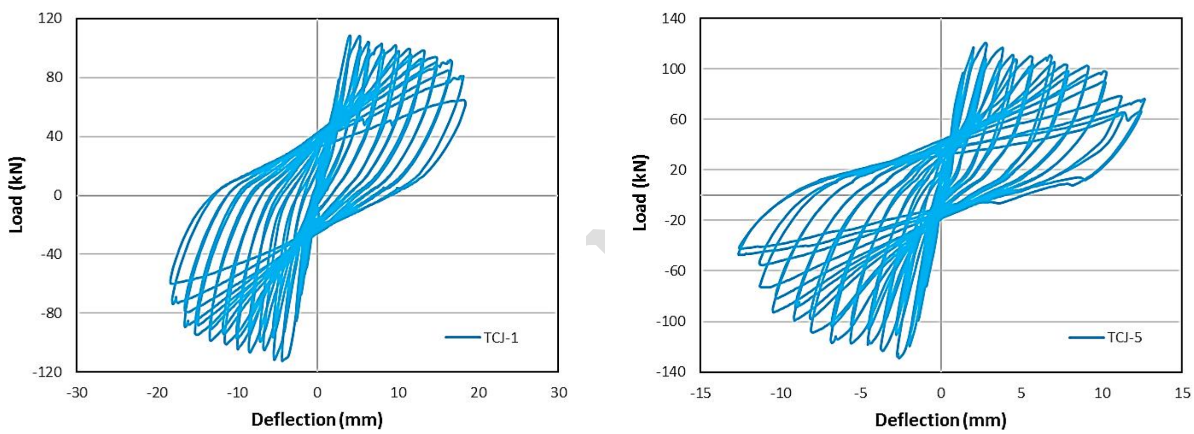

(a) (b)

Figure 4. Hysteresis load-deflection diagram for joint model (a) TCJ-1 and (b) TCJ-5

Based on the numerical results in Figure 5, increasing the wall thickness of the steel tube in the T-shaped connections has a small effect on improving the load-bearing capacity of this type of connection. However, by comparing the area under the hysteresis curves, it is clear that with increasing the wall thickness of the steel tube, the energy absorption rate increases significantly. For example, by increasing the wall thickness of the brace member in the composite connection from 4.2 to 6 mm, it was observed that the maximum load increased by 7.5%. This can be seen by comparing Figure 5. Accordingly, the ultimate load of the TCJ-2 connection model increased by 10.8 to 116.6 kN compared to the TCJ-1 connection. It is worth noting that the thickness of the steel brace wall in the TCJ-1 and TCJ-2 composite connections is 4.2 and 6 mm, respectively. Therefore, a 43% increase in thickness leads to a 7.5% increase in the load-bearing capacity in connections with a core concrete with a strength of 30 MPa. Considering economic considerations, this increase is insignificant.

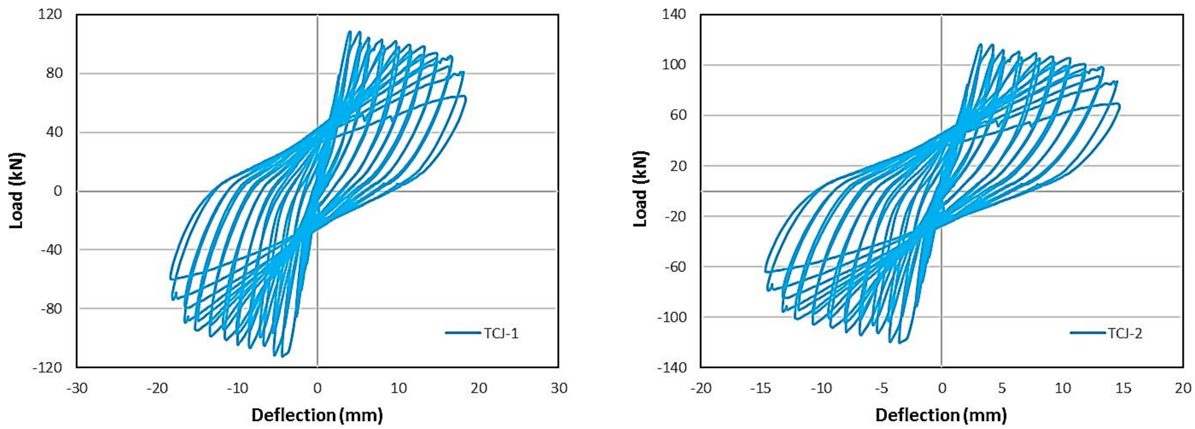

(a) (b)

Figure 5. Hysteresis load-deflection diagram for joint model (a) TCJ-1 and (b) TCJ-2

In addition, increasing the thickness of the steel wall also has a significant effect on improving the elastic stiffness and reducing the displacement of the connection. For example, the elastic stiffness of the numerical models has increased with increasing wall thickness.

5.4 Effect of Brace Section Dimension

The following discussion examines the effect of changes in the internal dimension of the brace member in the T-shaped connection and its effect on the desired parameters. According to Figure 6, the analysis of the numerical results shows that increasing the internal dimension of the brace leads to a significant increase in the bearing capacity of the connection and a significant improvement in the elastic stiffness of the T-shaped connections. Another important point is that by comparing the graphs in this section, it is clear that the effect of increasing the internal dimension of the brace in numerical models with higher wall thickness is greater and more visible. Regarding the joint model TCJ-3, it can be said that the difference between this connection and the joint model TCJ-1 is the increase in the brace dimension in the CFST connection by 66% from 60 to 100 mm. The ultimate load of the joint model TCJ-3 is 181.1 kN, which has increased by 67% compared to model TCJ-1. Additionally, the maximum displacement of the joint TCJ-3 is 11 mm, which is a 39% reduction compared to the TCJ-3 with a maximum displacement of 18 mm. This reduction is also 21% compared to model TCJ-2.

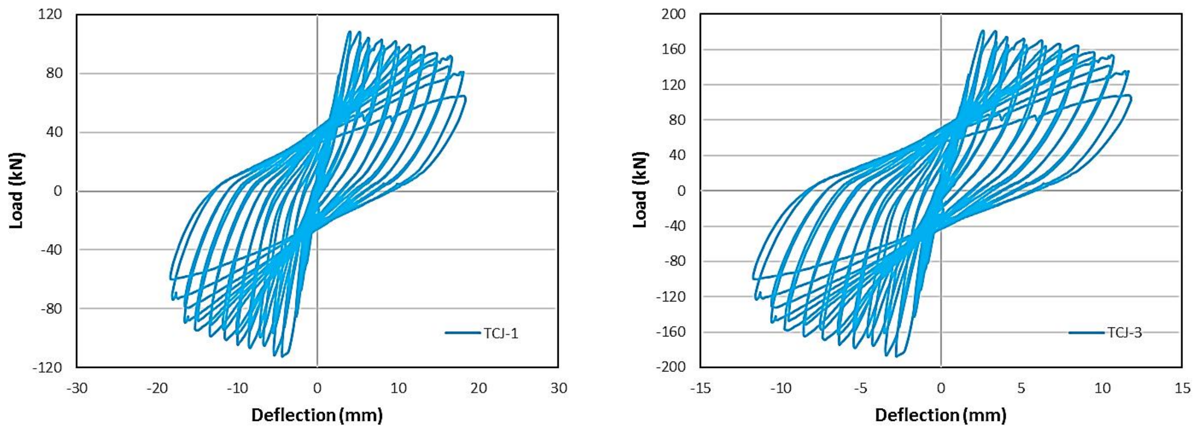

(a) (b)

Figure 6. Hysteresis load-deflection diagram for joint model (a) TCJ-1 and (b) TCJ-3

Furthermore, the joint model TCJ-4 is a connection model with a core concrete compressive strength of 30 MPa, a steel brace dimension of 100 mm, and a wall thickness of 6 mm. It can be seen that with a 43% increase in wall thickness and a 66% increase in cross-sectional dimension, the maximum load has increased from 108.5 kN to 194.8 kN, as shown in Figure 7. This increase in load capacity is equivalent to 79%. In addition, the maximum displacement in this connection model has decreased from 18 mm to about 10 mm compared to the reference model, which is equivalent to a 55% decrease.

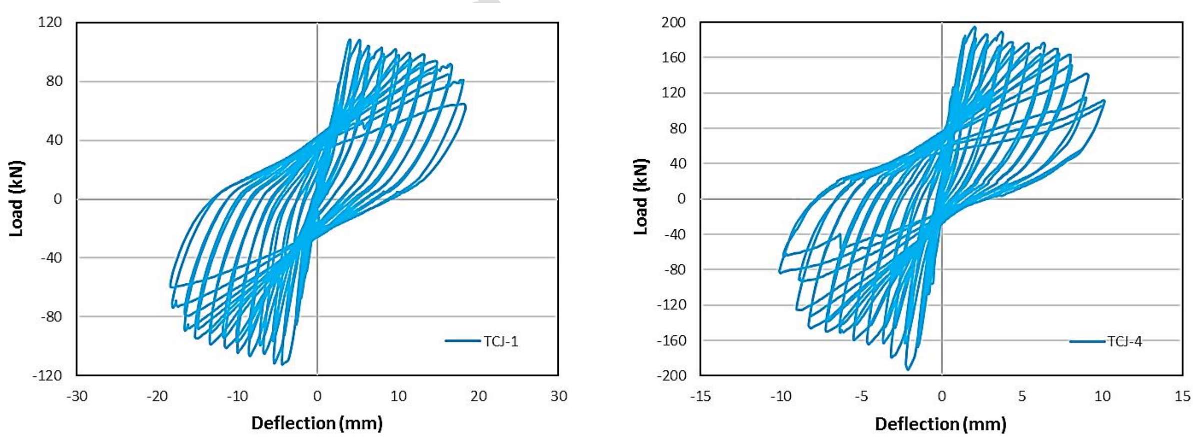

(a) (b)

Figure 7. Hysteresis load-deflection diagram for joint model (a) TCJ-1 and (b) TCJ-4

In the following part of the modeling results, the results of CFST T-joints with concrete grade 60 MPa are analyzed. By increasing the thickness of the brace member, the load has increased from 120.5 kN in model TCJ-5 to 131.3 kN in model TCJ-6. Also, the maximum displacement of the connection has decreased by 9.2% from 13 mm to 11.8 mm, as shown in Figure 8.

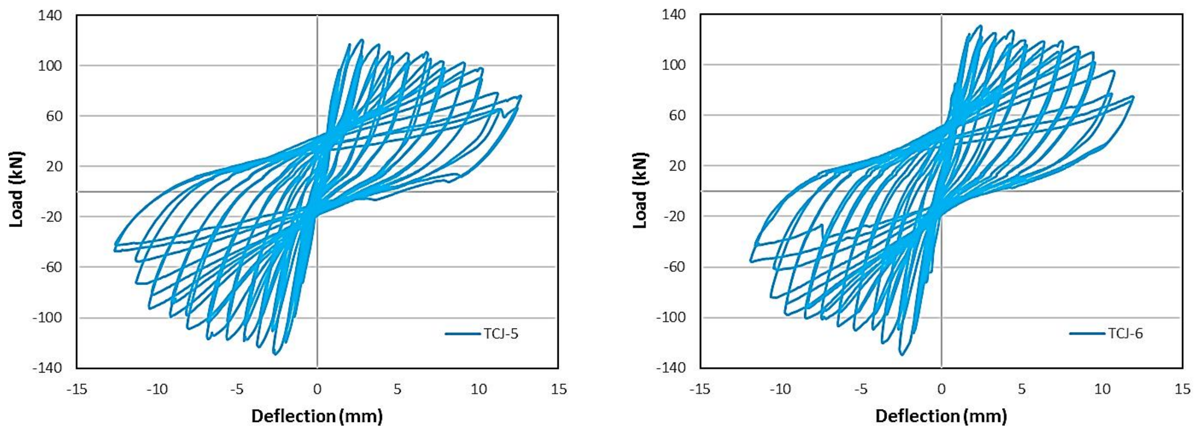

(a) (b)

Figure 8. Hysteresis load-deflection diagram for joint model (a) TCJ-5 and (b) TCJ-6

Additionally, the load-displacement diagram of the joint model TCJ-7 is shown in Figure 9-a. By comparing this diagram with other diagrams, it can be seen that the load capacity of this model is 192.8 kN. This model has a brace dimension and thickness of 100 mm and 4.2 mm. Also, the hysteresis diagram of model TCJ-8 with a concrete compressive strength of 60 MPa, a brace wall thickness of 6 mm and a dimension of 100 mm is shown in Figure 9-b. The load capacity of this connection is 210 kN and the maximum displacement is 7 mm.

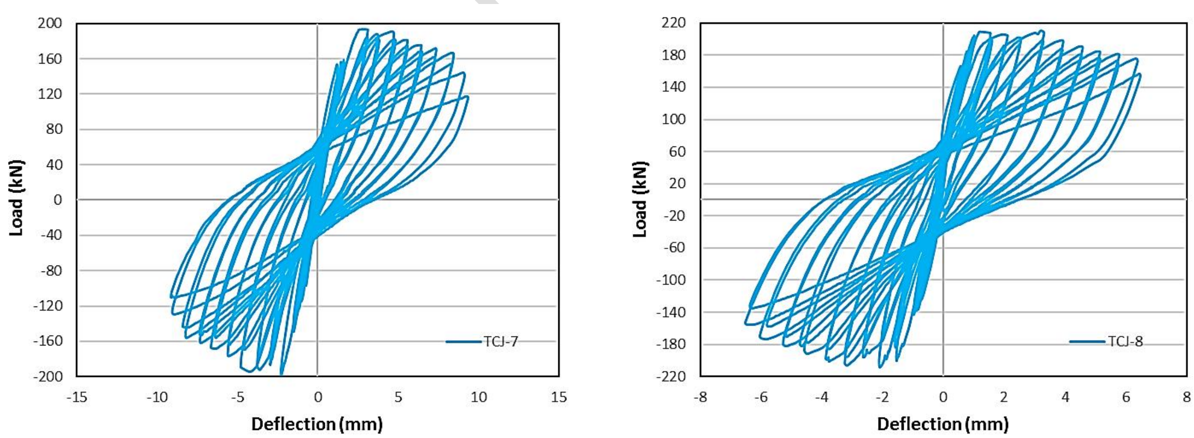

(a) (b)

Figure 9. Hysteresis load-deflection diagram for joint model (a) TCJ-7 and (b) TCJ-8

Numerical simulations reveal that CFST joints exhibit significant hysteretic energy dissipation under cyclic seismic loading, attributable to both steel yielding and concrete cracking/crushing. The confinement provided by the steel tube delays local buckling, allowing the joint to undergo large inelastic deformations before strength degradation becomes critical. The hysteresis loops generated in load-deflection space demonstrate stable energy dissipation in the initial cycles, followed by progressive pinching and degradation as damage accumulates. These findings have been captured in the comparison curves of all numerical joint models provided in Figure 10 for both concrete grades of 30 MPa and 60 MPa.

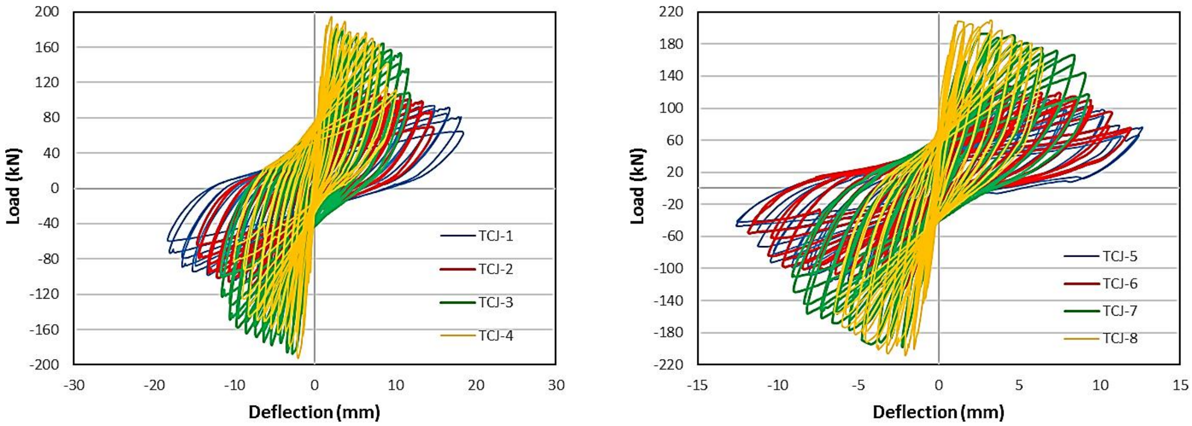

(a) (b)

Figure 10. Hysteresis load-deflection comparison for joint models with concrete grade (a) 30 MPa and (b) 60 MPa

5.5 Ductility and Hysteresis Damping

Table 4 summarizes the extracted ductility (μ) and equivalent viscous damping ratio (ζ_{hyst}) for all eight CFST T-joint models. The ductility values range from 2.8 to 4.2, indicating moderate to good seismic performance. Models with larger brace dimensions (TCJ-3, TCJ-4, TCJ-7, TCJ-8) exhibit higher ductility due to improved confinement and delayed local buckling. Hysteresis damping ranges from 8.5% to 12.3%, with larger brace sections providing greater energy dissipation capacity. The results confirm that increasing the brace dimension is the most effective strategy for enhancing both ductility and damping.

Table 4. Ductility and hysteresis damping parameters

Model ID	**Brace dimension, b_1 (mm)**	**Brace wall thickness, t_1 (mm)**	**Concrete strength, f_{cu} (MPa)**	**Ductility index, μ**	**Hysteresis damping ratio, ζ_{hyst} (%)**	**Energy dissipated (kN·mm)**
TCJ-1	60	4.2	30	2.8	8.5	425
TCJ-2	60	6.0	30	3.0	9.1	468
TCJ-3	100	4.2	30	3.9	11.2	712
TCJ-4	100	6.0	30	4.2	12.3	798
TCJ-5	60	4.2	60	2.9	8.8	445
TCJ-6	60	6.0	60	3.1	9.4	489
TCJ-7	100	4.2	60	4.0	11.5	738
TCJ-8	100	6.0	60	4.2	12.1	785

6. Discussion

6.1 Synthesis of parametric effects

The results demonstrate a clear hierarchy of parameter effectiveness: brace dimension, concrete strength, wall thickness. This hierarchy can be explained by fundamental mechanics. Increasing brace dimension (from 60 to 100 mm) directly increases the moment of inertia and section modulus, significantly enhancing flexural capacity. In contrast, increasing wall thickness primarily delays local buckling but does not substantially increase the elastic section modulus.

6.2 Comparison with existing literature

The finding that brace dimension is more effective than wall thickness is consistent with T-shaped composite joints, who observed a 47% capacity increase when β (b_1/b_0) increased from 0.3 to 0.5. The modest 11% increase from doubling concrete strength agrees with (Han, 2024), who noted that concrete strength effects are significant only in slender columns, not in joints.

6.3 Failure mechanisms

Qualitative observation of deformed shapes reveals that models with larger brace dimensions (100 mm) exhibit distributed plastic hinges at the brace-chord intersection, while models with smaller brace dimensions (60 mm) show localized chord face plastification. This distributed plasticity explains the higher ductility ($\mu = 4.2$ vs 3.0) and energy dissipation in larger-brace models.

6.4 Comparison with design codes

The predicted ultimate loads were compared with AISC 360-16 and EC4 design provisions. The numerical results are, on average, 15% higher than AISC predictions and 8% higher than EC4 predictions, indicating that current codes are somewhat conservative for CFST T-joints under cyclic loading.

6.5 Limitations

This study has several limitations: (1) Perfect bond without slip was assumed; (2) Only square sections were considered; (3) A single cyclic loading protocol (ATC-24) was used; (4) No thermal or fire effects were considered.

6.6 Sensitivity analysis

A sensitivity analysis was performed on the friction coefficient ($\mu = 0.1, 0.2, 0.3, 0.4$) and effective chord length ($L_0 = 600, 740, 900$ mm). The ultimate load varied by less than 3% across all friction coefficient values, indicating that the results are insensitive to this parameter within the typical range. Effective chord length had a more noticeable effect: reducing L_o from 740 to 600 mm increased stiffness by 8% but did not affect ultimate load. The baseline values ($\mu = 0.2$, $L_o = 740$ mm) are therefore appropriate.

7. Conclusions

The present study investigated the effect of mechanical and geometric variables on the seismic response of CFST T-shaped square-section joints filled with concrete under cyclic loading using the Abaqus software. Numerical models were evaluated in terms of ultimate load, overall joint stiffness, ductility, and energy absorption. The effect of core concrete strength, brace wall thickness, and section dimension on the load-bearing capacity of the joint models were discussed. Based on the results, the following conclusions can be drawn.

- The effect of increasing the brace dimension in numerical models with higher wall thickness is more pronounced.
- Increasing the brace wall thickness does not have a significant effect on improving the load-bearing capacity of T-shaped joints. However, increasing the wall thickness plays a role in improving the elastic stiffness and reducing the displacements of the connection.
- Increasing the brace dimension causes a significant increase in the load-bearing capacity and a significant improvement in the elastic stiffness of the T-shaped connections. Also, the effect of increasing the brace dimension is more significant compared to the wall thickness of the beam. For example, increasing the thickness by 43% causes only a 7.5% increase in the load-bearing capacity. This is while increasing the member dimension by 66% causes a 67% increase in the ultimate capacity of the joint.
- The effect of wall thickness is less compared to concrete strength. Increasing concrete strength by a factor of two increases the load-bearing capacity by 11%. Meanwhile, doubling the wall thickness in the CFST T-joint increases the ultimate capacity of the connection by approximately 9%.
- Increasing the brace dimension, increasing the concrete strength of the chord member, and then increasing the brace wall thickness, respectively, have the greatest increasing effect on the load-bearing capacity of the CFST T-joint connection.
- Limitations of this study: The numerical models assumed perfect bond between steel and concrete; did not consider weld geometric imperfections or residual stresses; used a single cyclic loading protocol; and only examined square sections.
- Recommendations for future work: Future research should (1) experimentally validate the numerical findings; (2) investigate the effect of width-to-thickness ratios (b_0/t_0 and b_1/t_1); (3) examine CFST T-joints under combined axial, bending, and cyclic loading; (4) develop design equations for ductility and energy dissipation; and (5) extend the analysis to circular and rectangular sections.

8. Acknowledgments

The authors acknowledge the use of AI-assisted language editing tools for improving the readability and grammar of this manuscript. All technical content, analysis, results, and conclusions remain the sole responsibility of the authors.

References

Abedini, F., Rafiee-Dehkharghani, R., & Laknejadi, K. (2025). Topology Optimization of Wave Barriers for Mitigating Dynamic Compaction-Induced Vibrations Using a Coupled CMA-ES/Finite-Element Method. *Civil Engineering Infrastructures Journal*, *58*(2), 369–389. https://doi.org/10.22059/ceij.2024.369737.1998

Ali, A., & Mahdi, F. (2025). Experimental Investigation of Short Concrete-Filled Lightly Reinforced RPC Compression Members under Edge Load. *Civil Engineering Infrastructures Journal*. https://doi.org/10.22059/ceij.2025.383449.2168

Ghandi, E., Mohammadi Rana, N., & Esmaeili Niari, S. (2025). Parametric Analysis of Axially Loaded Partially Concrete-Filled Cold-Formed Elliptical Columns Subjected to Lateral Impact Load. *Civil Engineering Infrastructures Journal*, *58*(1), 49–70. https://doi.org/10.22059/ceij.2024.364758.1955

Ghassemieh, M., Saneeinia, Z., & Baei, M. (2017). Concrete filled tubular bracing subjected to cyclic loading. *Civil Engineering Infrastructures Journal*, *50*(1), 165–177. https://doi.org/10.7508/ceij.2017.01.010

Han, L.-H. (2024). *Theory of concrete-filled steel tubular structures*. Springer.

Hassam, M., Guo, L., & Tahir, M. (2024). Strengthening schemes of special-shaped concrete-filled steel tubes: A review. Structures,

Huang, W., Fenu, L., Chen, B., & Briseghella, B. (2018). Experimental study on joint resistance and failure modes of concrete filled steel tubular (CFST) truss girders. *Journal of Constructional Steel Research*, *141*, 241–250.

ISLAM, M. M., Sen, D., & CHOWDHURY, S. R. (2024). Finite Element Analysis on The Effect of Gap Between Masonry Infill and Reinforced Concrete Frame Under Inplane Loading. *Civil Engineering Infrastructures Journal*. https://doi.org/10.22059/ceij.2024.375383.2055

Labibzadeh, M., Kordi, M., Hosseinlou, F., Rezaeian, A., & Khayat, M. (2024). Optimizing the performance of L-shaped concrete-filled steel tube columns under eccentric loading. *Civil Engineering Infrastructures Journal*. https://doi.org/10.22059/ceij.2024.372952.2018

Lan, X., Wang, Y., Tan, B., & Zhang, Y. (2024). An assessment of application of the component-based method to full range behaviour of joints between steel beam to concrete filled steel tube columns under extreme loading conditions. *Engineering Structures*, *309*, 118057. https://doi.org/10.1016/j.engstruct.2024.118057

Li, W., Xu, L.-F., & Qian, W.-W. (2021). Seismic performance of 3-D steel beam to concrete-encased CFST column joints: Tests. *Engineering Structures*, *232*, 111793. https://doi.org/10.1016/j.engstruct.2020.111793

Liang, Z.-S., & Han, L.-H. (2025). Performance of trussed concrete-filled steel tubular (CFST) hybrid structures subjected to eccentric compression. *Engineering Structures*, *334*, 120068. https://doi.org/10.1016/j.engstruct.2025.120068

Mashiri, F. R., & Zhao, X.-L. (2010). Square hollow section (SHS) T-joints with concrete-filled chords subjected to in-plane fatigue loading in the brace. *Thin-Walled Structures*, *48*(2), 150–158. https://doi.org/10.1016/j.tws.2009.07.010

Mofid, T., & Tavakoli, H. (2021). Experimental Investigation of Cyclic Degradation of Light RC Beams under Periodic Loading. *Journal of Structural and Construction Engineering*, *8*(Special Issue 2), 243–263. https://doi.org/10.22065/jsce.2020.217276.2060

Mofid, T., & Tavakoli, H. (2023). Experimental investigation of mechanical behavior of lightweight RC elements under repeated loadings. Structures,

Montuori, R., Nastri, E., Piluso, V., & Todisco, P. (2024). Finite element analysis of concrete filled steel tubes subjected to cyclic bending. *Engineering Structures*, *314*, 118364. https://doi.org/10.1016/j.engstruct.2024.118364

Nassiraei, H., Lotfollahi-Yaghin, M. A., & Ahmadi, H. (2016). Static strength of collar plate reinforced tubular T/Y-joints under brace compressive loading. *Journal of Constructional Steel Research*, *119*, 39–49. https://doi.org/10.1016/j.jcsr.2015.12.011

Omranian, E., Abdollahzadeh, G., Amiri, J. V., & Abdelnaby, A. E. (2023). Multiple earthquake effects on vulnerability of horizontally curved RC bridges. *Journal of earthquake engineering*, *27*(3), 597–622. https://doi.org/10.1080/13632469.2022.2030432

Pinto, C., & Fonseca, J. (2024). The mechanical behavior of high-strength concrete-filled steel tubes: a review. *CivilEng*, *5*(3), 591–608.

SHAHRIARI, A. R., & JAVAHERI, T. M. (2017). Cyclic loading tests for cold-formed steel wall frames with lightweight concrete. https://doi.org/10.7508/ceij.2017.01.007

Tavakoli, H. R., Mofid, T., & Dehestani, M. (2023). Dynamic analysis of thermal crack propagation in RCD dams considering rotational component of ground motion. https://doi.org/10.21203/rs.3.rs-2848554/v1

Varma, A. H., Ricles, J. M., Sause, R., & Lu, L.-W. (2004). Seismic behavior and design of high-strength square concrete-filled steel tube beam columns. *Journal of Structural Engineering*, *130*(2), 169–179.

Xie, K., Wang, H., Pang, J., & Zhou, J. (2019). Study of the ultimate bearing capacity of concrete-filled steel tube K-joints. *KSCE Journal of Civil Engineering*, *23*(5), 2254–2262. https://doi.org/10.1007/s12205-019-1268-7

Xie, W.-C., Jiang, H., Ye, Y., Liu, Y., & Xiang, Z.-H. (2025). Tensile performance of concrete-filled plastic-lined steel tube (CFPLST) T-shaped joints. *Journal of Constructional Steel Research*, *234*, 109739.

Xiong, M.-X., Pi, P.-W., & Long, Y.-L. (2025). Continuity of seismic performance of concrete-filled steel tubular columns across strength sequence variation from NSC through HSC to UHSC. Structures,

Xiong, M.-X., Ren, T., Zhou, P., Yang, M., Gong, W., & Li, H. (2024). Post-fire compressive behavior of CFRP stirrups reinforced CFST columns: Experimental investigation and calculation models. *Thin-Walled Structures*, *198*, 111747. https://doi.org/10.1016/j.tws.2024.111747

Yang, C., Chen, H., & Ou, J. (2024). Seismic behavior of composite bolted T-shaped exterior joints in modular steel construction. *Journal of Constructional Steel Research*, *212*, 108249. https://doi.org/10.1016/j.jcsr.2023.108249

Zhang, J.-c., Jiang, X.-g., Jia, Z.-k., Cao, M.-s., & Jia, J.-q. (2024). Seismic behavior of steel reinforced ultra-high strength concrete composite frame: Experimental and numerical study. *International Journal of Concrete Structures and Materials, 18*(1), 43. https://doi.org/10.1186/s40069-024-00685-w